Petroleum and Coal

Article **Open Access**

Natural Convective Non-Newtonian Casson Fluid Flow in a Porous Medium with Slip and Temperature Jump Boundary Conditions

Adebowale Martins Obalalu[1], Olusegun Adebayo Ajala[2], Adeshina Taofeeq Adeosun[3], Fatai Adisa Wahaab[4], Oluwaseyi Aliu[4], and Lawal Lanre Adebayo[4]*

[1] *Department of Statistics and Mathematical Sciences, Kwara State University, Malete, Nigeria*
[2] *Department of Pure and Applied Mathematics, Ladoke Akintola University of Technology, Ogbomoso, Nigeria*
[3] *Department of Mathematics, University of Ilorin, Ilorin, Nigeria*
[4] *Fundamental and Applied Science Department, Universiti Teknologi PETRONAS, Bandar Seri Iskandar, Malaysia*

Received July 14, 2019; Accepted November 25, 2020

Abstract

In this study, a two-dimensional hydromagnetic radiative non-newtonian Casson fluid flow through an oscillatory porous vertical channel has been studied. Using MATHEMATICA software, differential transform technique (DTM) is employed to solve the obtained dimensionless coupled non-linear ordinary differential equations. Differential transform method was used for the first time to solve the coupled nonlinear ordinary differential equations with slip and temperature jump boundary conditions. The transformed equations are controlled by the different parameters including temperature jump, radiation-conduction, Casson rheological, magnetic field, and porous medium. It is found that the fluid flow is depressed with magnetic field intensity while temperature was elevated. Temperature is found to be enhanced with temperature jump parameter. In addition, an increase in the Casson rheological has significant influence on the fluid flow. The findings from this study is relevant to enhance oil recovery.

Keywords: *Radiation-conduction; Differential transform method; Casson fluid; Temperature jump; Slip.*

1. Introduction

Hydromagnetic oscillatory flow has stimulated great interest due to its important function in many aspects of science and engineering such as electrical power generation, astrophysical flows, oil extraction, thermal insulation, heat exchange, and groundwater pollution [1-5]. Heat transfer is an important aspect of several fields involving the heating and cooling process. Hussain *et al.* [6] investigated the hall current effect on the natural convective heat transfer of an oscillating flow in a porous enclosure. The enhancement in the oscillation parameter was reported to have increased the fluid flow. In another hydromagnetic oscillatory fluid flow study in a saturated porous medium [7], the authors affirmed that the oscillation parameter reduces the temperature within the boundary layer. Another researcher has investigated the impact of radiating heat generated/absorbed in a saturated oscillating porous medium with slip and temperature jump effect [8]. The authors show that the heat generated/absorbed with the porous medium enhances the heat transfer wall. A further study investigated the heat transfer on a vertical channel as well as temperature jump in a porous medium [9]. The author reported a reduction in the fluid temperature jump during fluid absorption. Several analyses have been conducted on the effect of magnetohydrodynamic (MHD) oscillatory flow in porous media with slip and temperature jump effect [10-15]. Numerical simulation of hydromagnetic natural convective three-dimensional heat transfer with a magnetic field has also been studied [16]. Their report showed that the Lorentz force reduces the temperature gradient in natural convective flow. In another study of MHD oscillatory fluid flow of natural convection in a vertical porous

channel with a viscous dissipation effect [17], the authors showed that the fluid flow enhanced with an increase in the heat generation parameter. Another research group investigated the unsteady free convection over a stretching surface with the effect of velocity slip [18]. It was concluded that the thermal radiation parameter and temperature variations reduced the velocity profile.

The impact of the external magnetic field in an electrically conducting free convective fluid flow has played a significant role in numerous engineering and industrial applications [19-23]. This is due to the widespread in scientific and environmental processes such as MHD generator, geothermal energy extraction, purification of crude oil, electrical power generation, and astrophysical flows, aircraft propulsion devices, missiles and other military applications [24-30]. Obalalu *et al.* [31] reported the impact of the magnetic field on buoyancy-driven fluid flow in a rectangular cavity. The results showed that when electrically free convective fluid is irradiated by a magnetic field, Lorentz force becomes energetic and connects with buoyancy force resulting in a reduction in the fluid flow. Adesanya *et al.* [32] investigated the analytical expressions of magnetohydrodynamics free convective fluid flow through vertical parallel plates. The study involves the use of Joule dissipation effects employing A domain decomposition method to investigate and analyze the impact of MHD and thermal radiation on a vertical channel with time-periodic boundary conditions [33-35]. All aforementioned studies restricted their investigations to Newtonian natural convective heat transport/transfer.

Practically, a few non-Newtonian fluids behave like elastic solid such that once the shear stress is low, the fluid flow stops. The Casson fluid is a typical example of fluids with such behavior. The work of Casson [36] lay the foundation for non-Newtonian fluid flow studies. The study established the prediction of the flow behavior of pigment-oil suspension. The magnetohydrodynamic shearing property of the Casson fluid must surpass the yield shear stress. Casson model depends on a system of the joint reaction of solid and liquid, based on two-phase dissolution. In this regard, Hari and Harshad [19] studied the analytical expression of MHD Casson liquid flow on the oscillation vertical plate using the Laplace transform technique with the thermal radiation effect. Their results showed that the radiation parameter decreases the temperature and flow of the fluid. Another group has studied the effect of convective heating on non-Newtonian Casson fluid through a cramped stretching sheet [37-38]. Hari *et al.* [39] studied the Soret effect and numerical solution of hydromagnetic Casson fluid flow in an embedded porous medium. Boyd *et al.* [40] used the Lattice Boltzmann method to analyze non-Newtonian blood models on oscillating flow. Another research group studied the analytic expression and convective heating effect on the magnetohydrodynamics Casson fluid flow in an embedded porous medium [41]. Their results indicated that the Biot number enhanced the velocity of Casson fluid flow. Other researchers have investigated the analytical expression of stagnation point Casson fluid flow close to a stretching sheet using the homotopy analysis method [42], as well as the second law analysis of MHD Casson flow over a stretching sheet with velocity slip [43]. Their results revealed that the Casson parameter enhances the heat transfer wall.

Different methods including differential transform method (DTM) have been utilized in analyzing heat transfer in non-Newtonian Casson fluid flow. However, slip and temperature jump boundary condition have not been studied in semi-analytical DTM. In this study, a semi-analytical method, DTM, has been used to evaluate heat transfer of a Casson fluid flow in an unsteady oscillatory porous vertical channel with the introduction of slip and temperature jump boundary conditions. The findings from this study have a significant contribution to the existing knowledge and serve as a complement to past studies for practical applications such as oil recovery and food processing.

2. Mathematical model

We considered a Casson fluid flow of a free convective incompressible, electrically conducting, hydromagnetic in a vertically porous medium. Consideration is given to a free flow convective incompressible, hydromagnetic Casson fluid. The plates were subjected to steady periodic heating which leads to temperature gradient of the fluid, thereby setting the fluid in

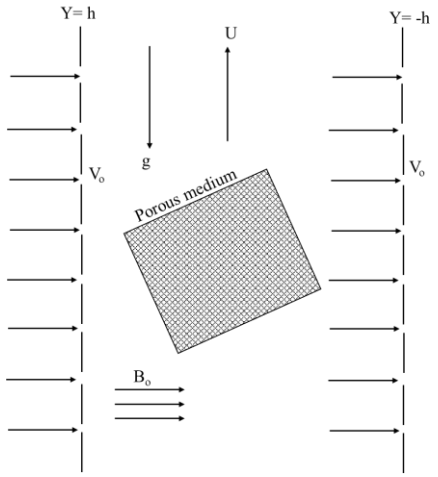

Figure 1. Illustration of the vertically oriented porous plate

motion. From this assumption, one porous plate (y=-h) was subjected to suction, while the other porous plate (y=+h) was subjected to injection. The low wall was heated with slip and temperature jump. The porous plate was taken vertically parallel to the x-axis at $y = \pm h$ as shown in Figure 1.

For Casson fluid, the constituting equations of isotropic and oscillatory flow can be expressed as [3, 14, 10].

$$\left.\begin{aligned}\tau_{ij} &= 2\left(\mu_B + \frac{P_y}{\sqrt{2\pi}}\right)e_{ij} \text{ when } \pi > \pi_c \\ \tau_{ij} &= 2\left(\mu_B + \frac{P_y}{\sqrt{2\pi c}}\right)e_{ij} \text{ when } \pi < \pi_c\end{aligned}\right\} \quad (1)$$

where. P_y is the fluid yield stress of liquid; τ_{ij} is the component of the stress tensor; μ_B is the plastic dynamic viscosity of the non-Newtonian fluid; $\pi = e_{ij}e_{ij}$ represent the product of the rate of strain tensor with itself; and π_c is the critical value of the product of the rate of strain tensor with itself.

The modified governing equations are [7, 9, 32].

$$\frac{\partial u'}{\partial t'} - v_0\frac{\partial u'}{\partial y'} = \frac{\mu_B}{\rho}\left(1+\frac{1}{c}\right)\frac{\partial^2 u'}{\partial y'^2} + g\beta(T-T_0) - \frac{\sigma B_0^2 u'}{\rho} + \frac{\mu_B}{\rho}\left(1+\frac{1}{c}\right)\frac{u'}{k} \quad (2)$$

$$\frac{\partial T}{\partial t'} - v_0\frac{\partial T}{\partial y'} = \frac{k}{\rho C_p}\frac{\partial^2 T}{\partial y'^2} + \frac{Q}{\rho C_p}(T_0 - T) - \frac{1}{\rho C_p}\frac{\partial q_r}{\partial y'} + \frac{\sigma B_0^2}{\rho C_p}u'^2 + \frac{\mu_B}{\rho C_p}\left(1+\frac{1}{c}\right)\left(\frac{\partial u'}{\partial y'}\right)^2 + \frac{\mu_B}{\rho C_p}\left(1+\frac{1}{c}\right)\frac{u'^2}{K} \quad (3)$$

with initial condition

$$u'(t',y') = 0, T(t',y') = 0 \quad at \quad t' = 0 \quad (4)$$

For rarefied flow with temperature jump, the fitting boundary condition can be expressed as

$$u'(t',y') = \frac{2-\xi}{\xi}\gamma\frac{\partial u'}{\partial y'} \quad (5)$$

$$T(t',y') = T_1 + T_2\cos(wt) + \frac{2-\sigma_T}{\sigma_T}\frac{2\psi}{\psi+1}\frac{\gamma}{P_r}\frac{dT}{dy'}, y' = -h \quad at \quad t' > 0 \quad (6)$$

The non-moving wall and isothermal condition gives

$$u'(t',y') = 0, T(t',y') = T_1 + T_2\cos(wt), \quad y' = h \quad at \quad t' > 0 \quad (7)$$

Using Roseland approximation, the radiative heat flux term can be expressed as

$$qr = -\frac{4\gamma'}{3\alpha'}\frac{\partial T^4}{\partial y'} \quad (8)$$

where: γ' and α' are Stefan Boltzman constant.

Assuming the difference with the flow are abundantly trivial such that T^4 can be described as a linear function of the temperature. This is achieved by expanding T^4 in a Taylor series about T and ignoring the higher-order terms, we get

$$T^4 = (4T_1)^3 T - 3T_1^4 \quad (9)$$

putting equation (8) and (9) into equation (3) gives

$$\frac{\partial T}{\partial t'} - v_0\frac{\partial T}{\partial y'} = \frac{K}{\rho C_p}\frac{\partial^2 T}{\partial y'^2} + \frac{Q}{\rho C_p}(T_0 - T) - \frac{16\gamma' T_1^3\partial^2 T}{3\alpha'\partial y'^2} + \frac{\sigma B_0^2}{\rho C_p}u'^2 + \frac{\mu_B}{\rho C_p}\left(1+\frac{1}{c}\right)\left(\frac{\partial y'}{\partial y'}\right)^2 + \frac{\mu_B}{\rho C_p}\left(1+\frac{1}{c}\right)\frac{u'^2}{K} \quad (10)$$

By solving equations (2)-(10), then equations (11) and (12) were used to split the velocity and temperature into a steady and unsteady part, respectively.

$$u'(t',y') = \frac{g\beta h^2}{\nu}\left((T_1 - T_0)A(y) + T_2 B(y)e^{i\omega t}\right) \quad (11)$$

$$T(t',y') = T_0 + (T_1 - T_0)F(y) + T_2 G(y)e^{i\omega t} \quad (12)$$

where $A(y)$ and $f(y)$ represents the steady part, whereas $B(y)$ and $G(y)$ represent the periodic parts of the velocity and temperature, accordingly. The dimensionless quantities are

$$y = \frac{y'}{h}, S_t = \frac{h^2\omega}{\nu}, P_r = \frac{\mu C_p}{k}, S = \frac{hv_0}{\nu}, \delta = \frac{Q_0 h^2}{k}, c = \frac{\mu_B\sqrt{2\pi}}{P_y}, K_n = \frac{\lambda}{h}\left(\frac{2-\sigma_t}{\sigma_t}\right)\frac{2\phi}{\phi+1}, \quad (13)$$

$$Da = \frac{k}{h^2}, \gamma = \frac{(2-\xi)\lambda}{\xi h}, H^2 = \frac{\sigma(B_0)^2 h^2}{\mu}, \beta = \frac{\sqrt{1}}{Da}, N = \frac{4\gamma^* T_1^3}{\alpha^* k}, E_c = \frac{g^2\beta^2 h^4}{k\nu}\rho(T_1 - T_0)$$

applying Equations (11)-(13) into Equations (2) and (3) and taking the order of e^{iwt}, nonlinear coupled ordinary differential equations was obtained as:

$$\left(1+\frac{1}{c}\right)A''(y) + SA' - A(y)\left(H^2 + \left(1+\frac{1}{c}\right)\beta^2\right) + F(y) = 0 \quad (14)$$

$$\left(\frac{1+4}{3}N\right)F''(y) + SP_r F'(y) - \delta F(y) + (\delta\beta^2 + H^2 E_c)\left(A(y)\right)^2 + \left(\left(1+\frac{1}{c}\right)\beta^2 Ec\right)F(y) = 0 \quad (15)$$

$$\left(1+\frac{1}{c}\right)B''(y) + SB' - \left(is_t + H^2 + \beta^2\left(1+\frac{1}{c}\right)\right)B(y) + G(y) = 0 \quad (16)$$

$$\left(\frac{1+4}{3}N\right)G''(y) + SP_r G'(y) - (is_t P_r + \delta)G(y) + (\delta\beta^2 + 2H^2 E_c)A(y)B(y) + \left(\left(1+\frac{1}{c}\right)\beta^2 Ec\right)G(y) = 0 \quad (17)$$

These equations were subjected to the boundary conditions highlighted in Equation (18).

$$A(-1) = \gamma A'(-1), A(1) = 0 \quad (18)$$

$$F(-1) = 1 + \frac{K_n}{P_r}F'(-1), F(1) = 1$$

$$B(-1) = \gamma B'(-1), B(1) = 0$$

$$G(-1) = 1 + \frac{K_n}{P_r}G'(-1), G(1) = 1$$

2.1. Analysis of differential transform method (DTM)

The main explanation and essential applications of differential transform method (DTM) were first proposed by Zhou [44]. The differential transform of the derivative of a function is defined as Equation (19).

$$U(k) = \frac{1}{k!}\left(\frac{d^k u(x)}{dx^k}\right)_{x=x_0} \quad (19)$$

where *u(x)* is the original function and *U(k)* is the transform function. The inverse differential transform of *U(k)* is given by Equation (20).

$$\mathrm{u(x)} = \sum_{\mathrm{k=0}}^{\infty}(\mathrm{x} - \mathrm{x_0})^{\mathrm{k}}\mathrm{U(k)} \quad (20)$$

In a real application, and when x_0 is chosen to be zero, then the function *u(x)* is expressed by a finite series and can be written as:

$$u(x) = \sum_{k=0}^{n} x^k U(k) \quad (21)$$

Table 1. Differential transform theorems [44]

Original functions	Transform functions
$F(y) = G(y) \pm H(y)$	$F(k) = G(k) \pm H(k)$
$F(y) = \lambda G(y)$	$F(k) = \lambda G(k)$
$F(y) = G(y)H(y)$	$F(k) = \sum_{i=0}^{k} G(k-i)H(i)$
$F(y) = \frac{d^n G(y)}{dy^n}$	$F(k) = \frac{(k+1)!}{k!} G(k+n)$
$F(y) = y^n$	$F(k) = \delta(k-n) = \begin{cases} 0 \; if \; k \neq n \\ 1 \; if \; k = n \end{cases}$

Taken differential transform of Equation (14)-(17) and using theorems in Table 1, , the following recurrence relationship was obtained.

$$\mathrm{A[k+2]} = \frac{1}{(\mathrm{k}+1)(\mathrm{k}+2)\left(1+\frac{1}{\mathrm{c}}\right)}\left\{\left(\mathrm{H^2A[k]} - \left(\left(1+\frac{1}{\mathrm{c}}\right)\beta^2\mathrm{A[k]} - \mathrm{F[k]} - (\mathrm{k}+1)\mathrm{A[k+1]S}\right)\right)\right\} \tag{22}$$

$$F[k+2] = \frac{1}{\left(\left(1+\frac{4}{3}R\right)(k+1)(k+2)\right)}\left(\delta F[k] - SPr(k+1)F[k+1] - H^2 Ec\sum_{i=0}^{k}(A[i]\,1 + \frac{1}{c}\right)Ec^2\left(\sum_{i=0}^{k}(A[i]A[k-i]) - \left(1+\frac{1}{c}\right)Ec^2\beta^2\sum_{i=0}^{k}(A[i]A[k-i])\right) \tag{23}$$

$$B[k+2] = \frac{1}{(k+1)(k+2)\left(1+\frac{1}{c}\right)}\left((H^2 + i\mathrm{St})B[k] - \left(\left(1+\frac{1}{c}\right)\beta^2\right)B[k] - (k+1)B[k+1]S - G[k]\right) \tag{24}$$

$$G[k+2] = \frac{1}{\left(\left(1+\frac{4}{3}R\right)(k+1)(k+2)\right)}(\mathrm{Pr}i\mathrm{St})G[k] + \delta G[k] - S\mathrm{Pr}(k+1)G[k+1] - (2H^2\mathrm{Ec})\sum_{i=0}^{k}(B[i] - \left(1+\frac{1}{c}\right)\mathrm{Ec}^2\beta^2\sum_{i=0}^{k}(B[i]B[k-i]) - \left(1+\frac{1}{c}\right)\mathrm{Ec}^2\beta^2\sum_{i=0}^{k}(B[i]B[k-i]) \tag{25}$$

The following series solutions are derived using Equation (21) and recurrence relations in Equations (22)-(25).

$$\mathrm{A(y)} = \mathrm{A[0]} + \mathrm{yA[1]} + \frac{\mathrm{y^2}\left(\mathrm{H^2A[0]} - \left(1+\frac{1}{\mathrm{c}}\right)\beta^2\mathrm{A[0]} - \mathrm{SA[1]} - \mathrm{F[0]}\right)}{2\left(1+\frac{1}{\mathrm{c}}\right)} - \frac{\mathrm{y^3}\left(\mathrm{H^2A[1]} - \left(1+\frac{1}{\mathrm{c}}\right)\beta^2\mathrm{A[1]} - \frac{\mathrm{S}\left(\mathrm{H^2A[0]} - \left(1+\frac{1}{\mathrm{c}}\right)\beta^2\mathrm{A[0]} - \mathrm{SA[1]} - \mathrm{F[0]}\right)}{1+\frac{1}{\mathrm{c}}} - \mathrm{F[1]}\right)}{6\left(1+\frac{1}{\mathrm{c}}\right)} \tag{26}$$

$$(y) = \mathrm{F}[0] + \mathrm{yF}[1] + \left(\frac{\mathrm{y}^2\left(-\left(1+\frac{1}{\mathrm{c}}\right)\mathrm{Ec}^2\beta^2\mathrm{A}[0]^2 - \left(1+\frac{1}{\mathrm{c}}\right)\mathrm{Ec}^3\mathrm{H}^2\mathrm{A}[0]^4 + \delta\mathrm{F}[0] - \mathrm{PrSF}[1]\right)}{2\left(1+\frac{4\mathrm{R}}{3}\right)}\right) \left(\frac{\mathrm{y}^3(-2(1+\frac{1}{\mathrm{c}})\mathrm{Ec}^2\beta^2\mathrm{A}[0]\mathrm{A}[1] - 4(1+\frac{1}{\mathrm{c}})\mathrm{Ec}^3\mathrm{H}^2\mathrm{A}[0]^2\mathrm{A}[1]^2 + \delta\mathrm{F}[1]}{6\left(1+\frac{4\mathrm{R}}{3}\right)}\right) \quad (27)$$

$$\mathrm{B(y)} = \mathrm{B}[0] + \mathrm{yB}[1] + \frac{\mathrm{y}^2\left((\mathrm{H}^2 + \mathrm{iSt})\mathrm{B}[0] - \left(1+\frac{1}{\mathrm{c}}\right)\beta^2\mathrm{B}[0] - \mathrm{SB}[1] - \mathrm{G}[0]\right)}{2\left(1+\frac{1}{\mathrm{c}}\right)} \quad (28)$$

$$y^3\left(\frac{(H^2 + iSt)B[1] - \left(1+\frac{1}{c}\right)\beta^2 B[1] - \frac{S\left((H^2 + iSt)B[0] - \left(1+\frac{1}{c}\right)\beta^2 B[0] - SB[1] - G[0]\right) - G[1]}{1+\frac{1}{c}}}{6\left(1+\frac{1}{c}\right)}\right)$$

$$\mathrm{G(y)} = \mathrm{G}[0] + \mathrm{yG}[1] + \mathrm{y}^2(-2\mathrm{EcH}^2\mathrm{B}[0]^2 - 2(1+\frac{1}{\mathrm{c}})\mathrm{Ec}^2\beta^2\mathrm{B}[0]^2 + \frac{\mathrm{iPrStG}[0]}{2\left(1+\frac{4\mathrm{R}}{3}\right)} + \delta\mathrm{G}[0]\left(\mathrm{PrSG}[1]) + y^3(-4\mathrm{Ec}H^2B[0]B[1] - 4(1+\frac{1}{c})\mathrm{Ec}^2\beta^2B[0]B[1] + \frac{i\mathrm{PrSt}G[1]}{6\left(1+\frac{4R}{3}\right)} + \delta G[1] - 2\mathrm{Pr}S\right) \quad (29)$$

Using the boundary conditions the values of constants are achieved. The shear stress (τ) and the rate of heat transfer (Nu) at the walls can be determined from and $\left(1+\frac{1}{c}\right)\frac{dB(y)}{dy}$ and $\frac{dG(y)}{dy}$,respectively.

3. Results and discussion

MATHEMATICA computer package was used to write the program for the expression given by equations (25)-(28). The values of parameters such as viscous heating (Ec) = 1.0, heat generation parameter (δ) = 1.0, Knudsen number (Kn) = 0.005, thermal radiation (N) = 1, magnetic field or square of Hartmann number (H) = 1, porous medium (β) = 1, Prandtl number (P_r) = 1, suction/injection parameter (S) = 1, Strouhal number S_t = 1, Casson parameter (c) =0.1, are default values used in this study. These parameters are kept constant throughout the study, except when stated otherwise. From Table 2, Table 3, the magnitude of wall shear stress and heat transfer rate are more pronounced for Casson fluid with (Prandtl-number=0.71 air) compared with (Prandtl-number=7.0 water).

A rise in the value of Prandtl-number enhances the magnitude of wall shear stress. Whereas, the extent of heat transfer also increases the convection heat transfer and supply more to the fluid motion within the channel walls. We observed a slight reduction in the magnitude of wall shear stress and the extent of heat transfer with an increase in magnetic field intensity. Logically, the magnetic field produces an electromagnetic force that reduces the degree of heat transfer [32].

Table 2. Wall shear stress and rate of heat transfer for (Prandtl-number =7 Water)

C	Ec	H	R	S	Shear stress at the wall	Heat transfer rate
0.1	0.6	1.5	2	0.2	0.44582	2.47582
1.5	0.6	1.5	2	0.2	1.21991	4.75398
2.0	0.6	1.5	2	0.2	2.34611	5.63801

0.1	0.6	1.5	2	0.2	1.02994	2.96733
0.1	2.0	1.5	2	0.2	0.78514	1.96481
0.1	4.0	1.5	2	0.2	0.62557	1.83811
0.1	0.6	1.5	2	0.2	1.05474	2.88784
0.1	0.6	2.5	2	0.2	0.57733	1.91036
0.1	0.6	5.0	2	0.2	0.28147	3.95684
0.1	0.6	1.5	2	0.2	0.27336	2.39273
0.1	0.6	1.5	7	0.2	0.15063	2.08647
0.1	0.6	1.5	8	0.2	0.08415	0.05201
0.1	0.6	1.5	2	0.2	0.86361	2.67112
0.1	0.6	1.5	2	1.0	0.54719	1.54663
0.1	0.6	1.5	2	3.5	0.150803	0.21748

Table 3. Wall shear stress and rate of heat transfer for (Prandtl-number =0.71 Air)

C	E_c	H	R	S	Shear stress at the wall	Heat transfer rate
0.1	0.6	1.5	2	0.2	0.18584	4.3735
1.5	0.6	1.5	2	0.2	1.56323	6.11294
2.0	0.6	1.5	2	0.2	3.62141	7.24150
0.1	0.6	1.5	2	0.2	0.78634	1.15491
0.1	2.0	1.5	2	0.2	0.51921	2.37091
0.1	4.0	1.5	2	0.2	0.25211	3.18721
0.1	0.6	1.5	2	0.2	0.78155	3.56100
0.1	0.6	2.5	2	0.2	0.42938	2.37241
0.1	0.6	5.0	2	0.2	0.09673	1.18396
0.1	0.6	1.5	2	0.2	0.28344	4.42050
0.1	0.6	1.5	7	0.2	0.27336	3.39553
0.1	0.6	1.5	8	0.2	0.26822	1.41027
0.1	0.6	1.5	2	0.2	0.89596	5.80631
0.1	0.6	1.5	2	1.0	0.67843	4.18102
0.1	0.6	1.5	2	3.5	0.45758	3.04762

An increasing Eckert number decreases the wall shear stress. On the contrary, the higher value of the E_c number enhances the temperature distribution. In the case of (Prandtl-number =0.71 air) and (Prandtl-number =7 water), the wall shear stress and heat transfer rate reduce with a rise in the suction/injection parameter and thermal radiation parameter. Figure 2a exhibit the impact of the Casson fluid parameter on the fluid flow. It is noticed that an increase in Casson fluid parameter leds to an improvement in the fluid flow. As expected, increasing the Casson parameter reduces the fluid flow at the wall. It is found that adequate Casson liquid dissolves the response of the non-Newtonian action [41]. This suggests that the pure fluid will act as a Newtonian fluid. However, the Casson fluid flow for the boundary plate thickness is higher as compared to the Newtonian fluid. This can be attributed to the plasticity of Casson fluid [37]. Further, it is noted that a rise in the value of Casson liquid tends to reduce the plasticity of fluid rise. This behavior also generates more fluid flow to the boundary plate. On the contrary, an increase in Casson fluid parameter reduces the temperature profile as shown in Figure 2b. An increase in Casson fluid parameter is observed to reduce the shear stress at the wall (Figure 2c). An opposite behavior is observed in Figure 2d where an increase in Casson fluid parameter increases the wall heat transfer.

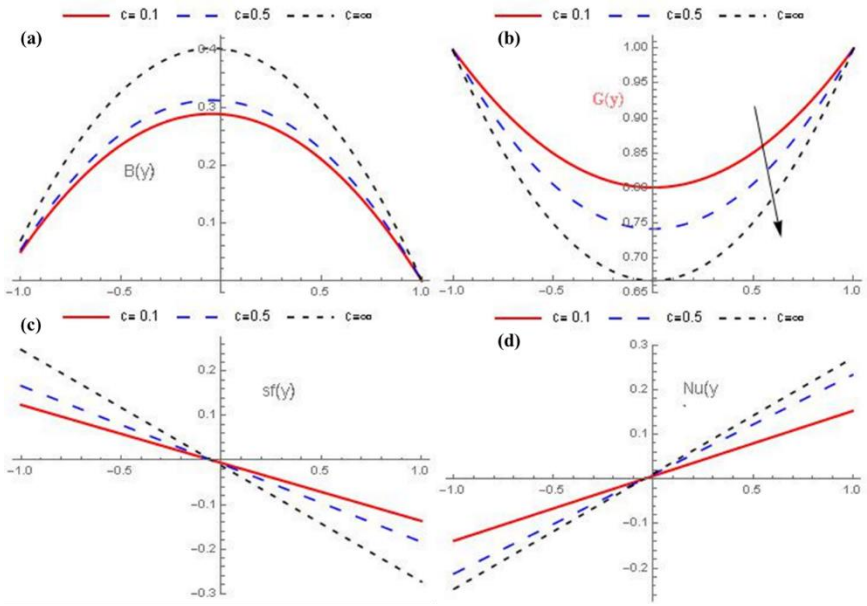

Figure 2. Impact of Casson fluid parameter on (a) fluid flow, (b) temperature profile, (c) shear stress at the wall, and (d) heat transfer wall

The Casson liquid performs effectively for transporting thermal energy with less shear stress within the boundary plate. Also, Casson fluid acquires high shearing within the fluid channel as the case with blood models [40]. Likewise, the Casson fluid parameter improved the rate of heat transfer to generate vasodilation [45]. Figure 3a presents the impact of magnetic field intensity on the Casson fluid velocity. It was noticed that an increase in the magnetic field tends to reduce fluid flow. Logically, opposing forces exist because of the existence of a magnetic field. Hence, it serves against the direction meanwhile its propensity to reduce and decelerate the Casson fluid motion [46]. In addition, an improvement in the magnetic field enhances the fluid temperature. Expectedly, the presence of Lorentz heating act as extra heat cause to the system fluid flow [31, 47]. Therefore, the effect of magnetic field intensity on the temperature profile can be attributed to the contribution of Lorentz heating as an extra heat source within the channel [24] as shown in Figure 3b. Table 4 present the convergence constants in which the presented DTM results show very good agreement with the past works [8, 17, 32].

Table 4. Convergence of constants a_0, a_1, f_0 and f_1 for $E_c = 0.1$, $H = 1$, $\delta = 1$, $P_r = 1$, $S = 1$ and $S_t = 1$, $c = \infty$, $\beta = 0$

N	a_0	a_1	f_0	f_1
1	0.00000	0.0000	1.00000	0.00000
2	0.22277	0.00000	0.66832	0.00000
3	0.21510	-0.04931	0.69724	0.08681
4	0.24176	-0.04277	0.66666	0.08273
5	0.23822	0.05428	0.67055	0.09269
6	0.24132	-0.05360	0.66857	0.09239
7	0.24092	-0.05469	0.66872	0.09278
8	0.24116	-0.05466	0.66876	0.09278
9	0.24113	-0.05472	0.66874	0.09272
10	0.24114	-0.05472	0.66876	0.09273
11	0.24114	-0.05472	0.66876	0.09272
12	0.24114	-0.05472	0.66876	0.09272
13	0.24114	-0.05472	0.66876	0.09272

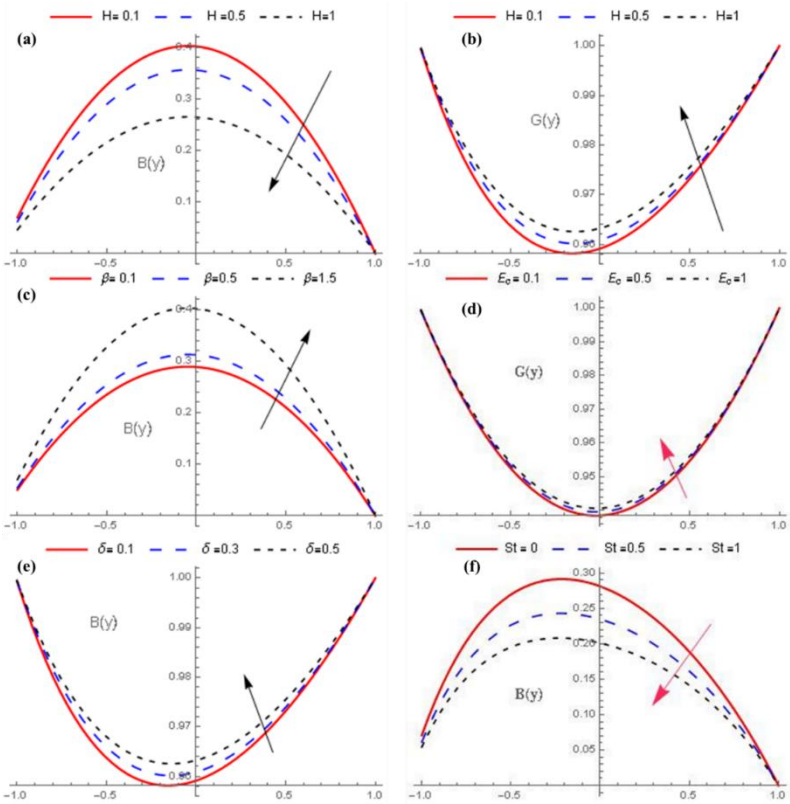

Figure 3. Impact of (a, b) magnetic field intensity on fluid flow and temperature profile, (c) porous medium on the fluid flow and temperature profile, (d) viscous dissipation in term of Eckert number on the fluid temperature (e) heat generation on the fluid temperature, (f) oscillation parameter on the fluid flow

Figure 3c presents the impact of the porous medium on the fluid flow. An increasing permeable medium enhances the porous channel on the fluid flow. Hence, the permeable medium favors the free flow of Casson fluid. Noticeably, an increase in viscous dissipation in terms of Eckert number enhances the fluid temperature. This described the physical case that as Eckert's number rise more thermal energy is supplied to increase the fluid temperature [8] so that the heat can conduct from the plate as shown in Figure 3d. Figure 3e present the effect of heat generation on the fluid temperature. It was noticed that a rise in heat generation enhances the temperature of the fluid. Physically, it may also be expected as the result of the heat source provide an increment in heat transfer. Figure 3f depicts the effect of the oscillation parameter on the fluid flow. An improvement in the oscillation parameter reduces the Casson fluid flow. Also, the strength of heating at the boundary plate reduces the heating magnitude.

Figure 4 shows the effect of the temperature jump parameter. It was noticed that an increase in the value of temperature jump parameters decreased the value of temperature profile during the fluid absorption. This can be ascribed to a rise in the particle space of the fluid as temperature jump increases [32, 48]. Hence, a reduction in the overall heat within the channel. Figure 4b exhibits the impact of suction/injection parameter on the Casson fluid flow. It was found that the fluid is uniform at the center of the channel. An increase in the suction/injection parameter within the channel also led to a rise of the suction/injection parameter at the wall. From Figure 4c, it was observed that the suction/injection parameter enhances the heated wall of the fluid temperature inside the channel. Moreso, the suction/injection parameter controls the hot fluid towards the direction of the cold wall. From Figure 4d, an increase in the thermal radiation parameter enhances the fluid temperature. It was found that the thermal radiation supplies higher heat to the fluid temperature. Consequently, the thermal radiation parameter described exactly the related additional conduction to the system [17].

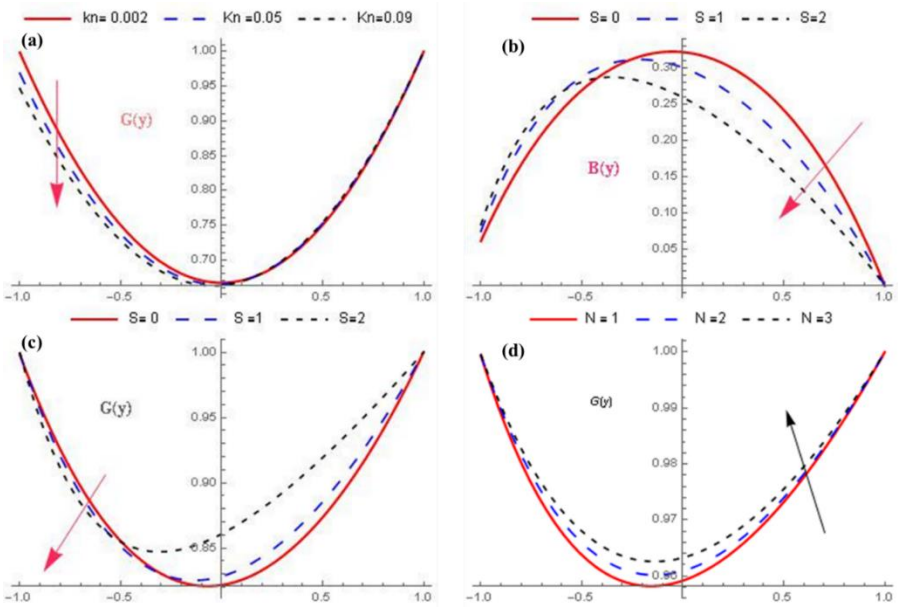

Figure 4. Impact of (a) temperature jump on temperature profile, (b, c) suction/injection parameter on the Casson fluid flow and heat wall, and (d) thermal radiation parameter on the fluid temperature

Figure 5a present the impact of the velocity slip parameter on the Casson fluid velocity. A rise in the velocity slip led to a rise in the velocity profile. The existence of a velocity slip was found to enhance the gas molecules' interaction [39, 49].

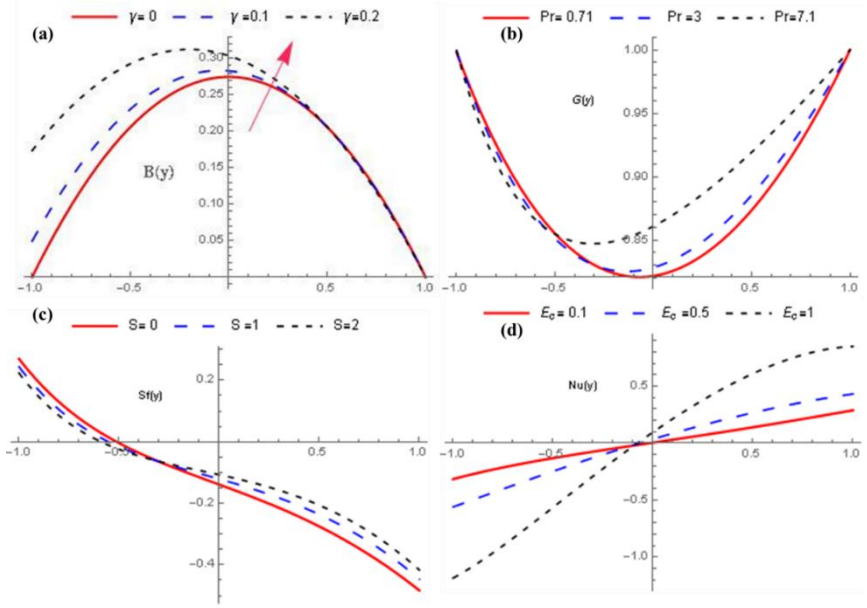

Figure 5. Impact of (a) velocity slip parameter Casson fluid velocity, (b) Prandtl number on fluid temperature, (c) suction/injection parameter on the wall shear stress, and (d) viscous dissipation in term of Eckert number on the heat transfer wall

Figure 5b presents the effect of the Prandtl number on fluid temperature. It was observed that an increase in the Prandtl number enhances the Casson fluid flow. The fluid thermal conductivity rises with (Prandtl number = 0.71 Air) to (Prandtl number = 7.1 water) which increases the boundary plate. This can be linked to a physical fact that as the Prandtl number increases the momentum to thermal diffusivities ratio, the fluid viscosity increases which are associated with fluid thickening and temperature distribution at the Walls [40, 50]. From Figure

5c, we observed a reduction in the suction/injection parameter on the wall shear stress. On the contrary, an increase in viscous dissipation in terms of Eckert number enhances the heat transfer wall as shown in Figure 5d.

Table 5 and Table 6 show the comparison of present results with previous studies when $\beta = 0$, $P_r = 1$, $H = 0$, $S = 0$, $\delta = 0$, $n = 15$, and Newtonian fluid ($c = \infty$), an excellent agreement can be observed.

Table 5. Comparison of results for f(y) with the previous works for: $\beta = 0$, $P_r = 1$, $H = 0$, $S = 0$ $\delta = 0$, $n = 15$, and Newtonian fluid ($c = \infty$)

y	Adesanya *et al.* [32]	Jha and Ajibade [17]	Gbedeyan *et al.* [41]	Present work
-1	1.0000	1.0000	1.0000	1.0000
-0.8	1.0050	1.0049	1.0050	1.0050
-0.6	1.0073	1.0073	1.0074	1.0074
-0.4	1.0082	1.0081	1.0083	1.0083
-0.2	1.0084	1.0083	1.0084	1.0084
0	1.0084	1.0083	1.0084	1.0084
0.2	1.0084	1.0083	1.0084	1.0084
0.4	1.0082	1.0081	1.0083	1.0083
0.6	1.0073	1.0073	1.0074	1.0074
0.8	1.0049	1.0049	1.0049	1.0049
1	1.0000	1.0000	1.0000	1.0000

Table 6. Comparison of results for A(y) with previous works for f(y) with the previous works for: $\beta = 0$, $P_r = 1$, $H = 0$, $S = 0$ $\delta = 0$, $n = 15$, and Newtonian fluid ($c = \infty$)

y	Adesanya *et al.* [32]	Jha and Ajibade [17]	Gbedeyan *et al.* [41]	Present work
-1	1.1096E-16	0.0000	0.0000	0.0000
-0.8	0.1813	0.1813	0.1813	0.1813
-0.6	0.3224	0.3224	0.3224	0.3224
-0.4	0.4232	0.4232	0.4232	0.4232
-0.2	0.4837	0.4837	0.4838	0.4838
0	0.5039	0.5039	0.5039	0.5039
0.2	0.4837	0.4837	0.4838	0.4838
0.4	0.4232	0.4232	0.4232	0.4232
0.6	0.3224	0.3224	0.3224	0.3224
0.8	0.1813	0.1813	0.1813	0.1813
1	9.7145E-15	0.0000	0.0000	0.0000

4. Conclusion

This study investigates the analytical expressions of an oscillatory, hydromagnetic, radiative non-Newtonian Casson fluid. A free convective, unsteady heat transfer with temperature jump and velocity slip using non-linear Differential transform method of solution (DTM) has been considered. The effect of various thermophysical parameters on Casson fluid velocity, fluid temperature, wall shear stress, and heat transfer wall is discussed. Results show that fluid flow improves with an increase in the values of *c* and *y*. Whereas, a reduction in the fluid flow was achieved with an increase in the values of *H, δ, St*, and *S*. An increase in *δ*, *Pr, Ec, c, H, β, N,* raise the fluid temperature. On the contrary, an increase in the K_n value reduces the fluid temperature. An increase in *Ec, H, N,* and *S* values slow down the wall shear stress while an increase in c tends to enhance the wall shear stress. A rise in the value of E_c and *c*, enhance the heat transfer wall while an increase in the values of *N, S*, and *H* leads to a reduction in the heat transfer wall. In summary, it is observed that the Casson parameter is inversely proportional to the yield stress. It is reasonable to conclude that the Differential transform method of solution (DTM) used in this study can be effectively employed to study heat transfer properties in physical, chemical, and biological sciences.

Nomenclature

E_c	*viscous heating parameter*	Q	*term due to internal heat generation*
λ	*molecular mean free path*	Φ	*specific heat ratio*
B_0	*magnetic field strength*	x	*vertical coordinate*
g	*gravitational acceleration*	H	*magnetic field parameter*
σ	*electrical conductivity*	T	*fluid temperature*
C_p	*specific heat capacity at constant pressure*	c	*Casson parameter*
ω	*frequency*	T_o, T_1, T_2	*reference fluid temperature respectively*
y	*horizontal coordinate*	K_n	*Knudsen number*
k	*thermal conductivity*	N	*radiation-conduction*
h	*half channel width*	γ	*Navier's slip parameter*
u'	*velocity*	S_t	*Strouhal number*
t'	*time*	P_r	*Prandtl number*
δ	*heat generation parameter*	N	*radiation-conduction*
ξ	*tangential momentum accommodation co-efficient intensity*	s	*suction/injection parameter*
β	*porous medium*		

Acknowledgment

The authors thank the staff and lecturers of Kwara State University, Malete, Kwara State, Nigeria for their kind support.

Conflict of interest

The authors declare none

References

[1] Chand K, Kumar R, and Sharma S. Hydromagnetic oscillatory flow through a porous medium bounded by two vertical porous plates with heat source and soret effect. Advances in applied Sciences Research, 2012; 3(4): 2169-2178.

[2] Hayat T, Nadeem S, Siddiqui AM, and Asghar l. An oscillating hydromagnetic non-Newtonian flow in a rotating system. Applied Mathematics Letters, 2004; 17(5): 609-614.

[3] Rauf A, Abbas Z, and Shehzad SA. Chemically Reactive Hydromagnetic Flow over a Stretchable Oscillatory Rotating Disk with Thermal Radiation and Heat Source/Sink: A Numerical Study. Heat Transfer Research, 2019; 50(15): 360-386.

[4] El-Hakiem M. MHD oscillatory flow on free convection–radiation through a porous medium with constant suction velocity. Journal of Magnetism and Magnetic Materials, 2000; 220(2): 271-276.

[5] Gandluru S, Prasada Rao DRV, and Makinde OD. Hydromagnetic-oscillatory flow of a nanofluid with Hall effect and thermal radiation past vertical plate in a rotating porous medium," Multidiscipline Modelling in Materials and Structures, 2018; 14(31):

[6] Hussain M, Hayat T, Asghar S, and Fetecau C. Oscillatory flows of second grade fluid in a porous space. Nonlinear Analysis: Real World Applications, 2010; 11(4): 2403-2414.

[7] Falade J, Ukaegbu JC, Egere A, and Adesanya SO. MHD oscillatory flow through a porous channel saturated with porous medium. Alexandria engineering journal, 2017; 56(1): 147-152.

[8] Titiloye E, Gbadeyan J, and Adeosun A. An oscillatory radiating hydromagnetic internal heat generating fluid flow through a vertcal porous channel with slip and temperature jump. International Journal of Applied Mechanics and Engineering, 2018; 23(2): 503-519.

[9] Adesanya SO. Free convective flow of heat generating fluid through a porous vertical channel with velocity slip and temperature jump. Ain Shams Engineering Journal, 2015; 6(3) 1045-1052.

[10] Khaled AR, and Vafai K. The effect of the slip condition on Stokes and Couette flows due to an oscillating wall: exact solutions. International Journal of Non-Linear Mechanics, 2004; 39(5): 795-809.

[11] Makinde OD, and Mhone P. Heat transfer to MHD oscillatory flow in a channel filled with porous medium. Romanian Journal of physics, 2005; 50(9/10): 931.

[12] Mehmood A, and Ali A. The effect of slip condition on unsteady MHD oscillatory flow of a viscous fluid in a planer channel. Romanian journal of physics, 2007; 52(1/2): 85.

[13] Kumar R. Influence of slip and jump boundary conditions on MHD oscillatory flow of radiating fluid through a vertical porous channel. Journal of Chemical, Biological and Physical Sciences (JCBPS), 2012; 2(2): 955.
[14] Sivaraj R, and Benazir AJ. Unsteady magnetohydrodynamic mixed convective oscillatory flow of Casson fluid in a porous asymmetric wavy channel. Special Topics & Reviews in Porous Media: An International Journal, 2015; (6)3. 267-281.
[15] Mehmood A, Ali A, and Mahmood T. Unsteady magnetohydrodynamic oscillatory flow and heat transfer analysis of a viscous fluid in a porous channel filled with a saturated porous medium. Journal of Porous Media, 2010; 13(6): 249-261.
[16] Sheikholeslami M, and Ellahi R. Three-dimensional mesoscopic simulation of magnetic field effect on natural convection of nanofluid. International Journal of Heat and Mass Transfer, 2015; 8(9): 799-808.
[17] Jha BK and Ajibade AO. Effect of viscous dissipation on natural convection flow between vertical parallel plates with time-periodic boundary conditions. Communications in Nonlinear Science and Numerical Simulation, 2012; 17(4): 1576-1587.
[18] Mukhopadhyay S, and Andersson HI. Effects of slip and heat transfer analysis of flow over an unsteady stretching surface. Heat and Mass Transfer, 2009; 45(11): 1447-1452.
[19] Kolsi L, Abidi A, Borjini NM, and Aïssia BH. The effect of an external magnetic field on the entropy generation in three-dimensional natural convection. Thermal Science, 2010; 14(2): 341-352.
[20] Mehrez Z, El-Cafsi A, Belghith A, and Le-Quéré P. MHD effects on heat transfer and entropy generation of nanofluid flow in an open cavity. Journal of Magnetism and Magnetic Materials, 2015; 3(7): 214-224.
[21] Rezaei G, and Karimi M. Third harmonic generation in a coaxial cylindrical quantum well wire: Magnetic field and geometrical size effects. Optics Communications, 2012; 285(24): 5467-5471.
[22] Chamkha AJ. Heat and mass transfer from a permeable cylinder in a porous medium with magnetic field and heat generation/absorption effects. Numerical Heat Transfer Part A- Applications, 2001; 40(4): 387-401.
[23] Aliu O, Sakidin H, Foroozesh J, and Yahya N. Lattice Boltzmann application to nanofluids dynamics-A review. Journal of Molecular Liquids, 2020; 300: 112-284.
[24] Ismail HNA, Abourabia AM, Hammad D, Ahmed NA, and El-Desouky A. On the MHD flow and heat transfer of a micropolar fluid in a rectangular duct under the effects of the induced magnetic field and slip boundary conditions. SN Applied Sciences, 2020; 2(1): 25.
[25] Zhang X, Mao J, Chen Y, Pan C, and Xu Z. Investigations of liquid metal magnetohydrodynamic rectangular duct flows under inclined transversal magnetic fields. Nuclear Fusion, 2019; 59(5): 056-018.
[26] Medebber MA, Aissa A, Slimani MEA, and Retiel N. Numerical Study of Natural Convection in Vertical Cylindrical Annular Enclosure Filled with Cu-Water Nanofluid under Magnetic Fields. Defect and Diffusion Forum, 2019; 3(2): 123-137.
[27] Malekan M, Khosravi A, and Zhao X. The influence of magnetic field on heat transfer of magnetic nanofluid in a double pipe heat exchanger proposed in a small-scale CAES system. Applied Thermal Engineering, 2019; 4(6): 146-159.
[28] Mehmood R, Nadeem S, and Masood S. Effects of transverse magnetic field on a rotating micropolar fluid between parallel plates with heat transfer, Journal of Magnetism and Magnetic Materials, 2016; 4(1): 1006-1014.
[29] Ellahi R. The effects of MHD and temperature dependent viscosity on the flow of non-Newtonian nanofluid in a pipe: analytical solutions. Applied Mathematical Modelling, 2013; 37(3): 1451-1467.
[30] Khan D, Khan A, Khan I, Ali F, ul-Karim F, and Tlili I. Effects of Relative Magnetic Field, Chemical Reaction, Heat Generation and Newtonian Heating on Convection Flow of Casson Fluid over a Moving Vertical Plate Embedded in a Porous Medium. Scientific reports, 2019; 9(1): 1-18.
[31] Obalalu AM, Wahaab FA, and Adebayo LL. Heat transfer in an unsteady vertical porous channel with injection/suction in the presence of heat generation. Journal of Taibah University for Science, 2020; 14(1): 541-548.
[32] Adesanya S, Oluwadare E, Falade J, and Makinde OD. Hydromagnetic natural convection flow between vertical parallel plates with time-periodic boundary conditions Journal of Magnetism and Magnetic Materials, 2015; 3(6): 295-303.

[33] Turkyilmazoglu M. Thermal radiation effects on the time-dependent MHD permeable flow having variable viscosity. International Journal of Thermal Sciences, 2011; 50(1): 88-96.
[34] Saleem M, Hossain M, Saha SC, and Gu Y. Heat transfer analysis of viscous incompressible fluid by combined natural convection and radiation in an open cavity. Mathematical Problems in Engineering, 2014; 412-480.
[35] Mondal S, Haroun NA, and Sibanda P. The effects of thermal radiation on an unsteady MHD axisymmetric stagnation-point flow over a shrinking sheet in presence of temperature dependent thermal conductivity with Navier slip, 2015; 10(9): 123-137.
[36] Casson N. A flow equation for pigment-oil suspensions of the printing ink type Rheology of disperse systems, 1959.
[37] Nadeem S, Haq RU, and Lee C. MHD flow of a Casson fluid over an exponentially shrinking sheet. Scientia Iranica, 2012; 19(6): 1550-1553.
[38] Nadeem S, Haq RU, Akbar NS, and Khan ZH. MHD three-dimensional Casson fluid flow past a porous linearly stretching sheet. Alexandria Engineering Journal, 2013; 52(4): 577-582.
[39] Kataria HR, and Patel HR. Soret and heat generation effects on MHD Casson fluid flow past an oscillating vertical plate embedded through porous medium," Alexandria Engineering Journal, 2016; 55(3) 2125-2137.
[40] Boyd J, Buick JM, and Green S. Analysis of the Casson and Carreau-Yasuda non-Newtonian blood models in steady and oscillatory flows using the lattice Boltzmann method. Physics of Fluids, 2007; 19(9): 093-103.
[41] Gbadeyan J, Titiloye E, and Adeosun A. Effect of variable thermal conductivity and viscosity on Casson nanofluid flow with convective heating and velocity slip. Heliyon, 2020; 6(1), 03076.
[42] Mustafa M, Hayat T, Ioan P, and Hendi A. Stagnation-point flow and heat transfer of a Casson fluid towards a stretching sheet. Zeitschrift für Naturforschung, 2012; 7(2): 70-76, 2012.
[43] Abd El-Aziz M, and Afify AA. MHD Casson fluid flow over a stretching sheet with entropy generation analysis and Hall influence. Entropy, 2019; 21(6) 592.
[44] Zhou J. Differential transformation and its applications for electrical circuits. ed: Huazhong University Press, Wuhan, China, 1986.
[45] Saidulu N, and Ventakata A. Slip effect on MHD flow of Casson fluid over an exponentially stretching sheet in the presence of thermal radiation, heat source/sink and chemical reaction. European Journal of Advances in Engineering and Technology, 2016; 55(3): 47-55.
[46] Shaw S, Mahanta G, and Sibanda J. Non-linear thermal convection in a Casson fluid flow over a horizontal plate with convective boundary condition. Alexandria Engineering Journal, 2016; 55(2): 1295-1304.
[47] Ajala OA, Obalalu AM, Abimbade SF, and Akinyemi OT. Numerical Study of Forced Convective Heat Generation Flow through a Permeable Walls with Suction/Injection. International Journal of Scientific and Research Publications (IJSRP), 2016; 9(6).
[48] Ajala OA, Adegbite P, Abimbade SF, and Obalalu AM. Thermal Radiation and Convective Heating on Hydro magnetic Boundary Layer Flow of Nanofluid past a Permeable Stretching Surface. International Journal of Applied Mathematics & Statistical Sciences, 2019: 4(6): 295-300.
[49] Makinde OD, and Chinyoka T. Numerical investigation of buoyancy effects on hydromagnetic unsteady flow through a porous channel with suction/injection Journal of Mechanical Science and Technology 2013; 27(5): 1557-1568.
[50] Ajala OA, Abimbade SF, Obalalu AM, and Adeosun A. Existence and uniqueness of forced convective flow through a channel with permeable walls in presence of heat generation. International Journal of Engineering Applied Sciences and Technology, 2019. 4(7): 194-197.

To whom correspondence should be addressed: Dr. Adebowale Martins Obalalu, Department of Statistics and Mathematical Sciences, Kwara State University, Malete, Nigeria,
E-mail: *adebowale.obalalu17@kwasu.edu.ng*